Stereointegrity of Tröger's Base: Gas-Chromatographic Determination of the Enantiomerization Barrier

Oliver Trapp and Volker Schurig*

Contribution from the Institut für Organische Chemie, Universität Tübingen, Auf der Morgenstelle 18, D-72076 Tübingen, Germany

Received April 14, 1999. Revised Manuscript Received November 19, 1999

Abstract: Tröger's base **1** (2,8-dimethyl-6*H*,12*H*-5,11-methanodibenzo[*b*,*f*][1,5]diazocine) undergoes enantiomerization in the gas and liquid phases. By enantioselective stopped-flow multidimensional gas chromatography, Eyring activation parameters of the enantiomerization barrier have been determined in the inert mobile gas phase (helium): $\Delta G^{\ddagger}_{gas}(298.15\ K) = 112.8 \pm 0.5$ kJ mol^{-1}; $\Delta H^{\ddagger}_{gas} = 62.7 \pm 0.3$ kJ mol^{-1}; $\Delta S^{\ddagger}_{gas} = -168 \pm 6$ J (K mol)$^{-1}$. An enantiomerization pathway proceeding via a degenerated retro-hetero-Diels−Alder ring opening or formation of a zwitterionic structure of **1** is proposed. By enantioselective dynamic gas chromatography, Eyring activation parameters have also been determined via computer-aided simulation of experimental interconversion peak profiles in the chiral stationary liquid phase: $\Delta G^{\ddagger}_{liq}(298.15\ K) = 117.8 \pm 0.5$ kJ mol^{-1}; $\Delta H^{\ddagger}_{liq} = 48.9$ kJ mol^{-1}; $\Delta S^{\ddagger}_{liq} = -231 \pm 8$ J (K mol)$^{-1}$. Surprisingly, in the presence of the chiral stationary phase (CSP) Chirasil-β-Dex, required for enantiomer separation of **1**, the enantiomerization barrier is higher than in the gas phase. The concept of the retention increment R' has been applied to distinguish the enantiomerization barrier of **1** in the dissolved and complexed state of the stationary phase.

1. Introduction

In 1890, Werner extended to trivalent nitrogen the widely accepted concept of van't Hoff and Le Bel on the tetrahedral tetravalent carbon.[1] In 1924, Meisenheimer et al. suggested that pyramidal inversion was responsible for the inability of trivalent nitrogen to display optical activity.[2] Indeed, several classical attempts to resolve racemic chiral tertiary amines of the type NXYZ, existing as rapidly interconverted invertomers (and hence inseparable enantiomers), failed until 1968. By linking lone-pair-containing atoms to nitrogen and by incorporation of stereogenic nitrogen into a constrained (three-membered) ring, the barrier of inversion is increased as demonstrated by the separation and isolation of stereoisomeric 1-chloroaziridines,[3] by complete resolution of 1-alkoxyoxazolidines,[4] and by enantiomeric or diastereomeric enrichment of dialkoxyamines, containing the asymmetric nitrogen solely in the open chain.[5] Another strategy toward stable stereogenic nitrogen relies on the design of molecular architectures containing trivalent nitrogen as a bridgehead. In 1887, Tröger isolated the bicyclic compound **1** (Figure 1), widely known as Tröger's base, via condensation of formaldehyde and *p*-toluidine.[6,7]

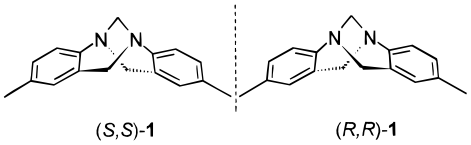

(*S*,*S*)-**1** (*R*,*R*)-**1**

Figure 1. Left: (5*S*,11*S*)-(+)-2,8-dimethyl-6*H*,12*H*-5,11-methanodibenzo-[*b*,*f*][1,5]diazocine,[8] (*S*,*S*)-**1**. Right: (5*R*,11*R*)-(−)-2,8-dimethyl-6*H*,12*H*-5,11-methanodibenzo[*b*,*f*][1,5]diazocine,[8] (*R*,*R*)-**1**.

The constitution of **1** was determined via degradation studies and by synthesis,[9,10] and various derivatives were obtained subsequently.[11] The inherent chirality of the heterocyclic amine

* Corresponding author. E-mail: volker.schurig@uni-tuebingen.de.

(1) Werner, A. *Über die räumliche Anordnung der Atome in stickstoffhaltigen Molekülen* (On the spatial arrangement of the atoms in nitrogen-containing molecules), Doctoral Thesis, Polytechnikum Zürich, 1890.

(2) (a) Meisenheimer, J.; Angermann, L.; Finn, O.; Vieweg, E. *Ber. Dtsch. Chem. Ges.* **1924**, *57*, 1747. (b) Meisenheimer, J.; Theilacker, W. In: *Stereochemie*; Freudenberg, K., Ed.; Deuticke: Leipzig-Wien, 1933; p 1147. (c) Lambert, J. B. *Top. Stereochem.* **1971**, *6*, 19−105.

(3) (a) Brois, S. J. *J. Am. Chem. Soc.* **1968**, *90*, 506, 508. (b) Lehn, J.-M.; Wagner, J. *J. Chem. Soc., Chem. Commun.* **1968**, 148. (c) Felix, D.; Eschenmoser, A. *Angew. Chem., Int. Ed. Engl.* **1968**, *7*, 224. (d) Kostyanovsky, R. G.; Samoilova, Z. E.; Chervin, I. I. *Bull. Acad. Sci. USSR, Div. Chem. Soc.* **1968**, 2705. (e) Schurig, V.; Bürkle, W.; Zlatkis, A.; Poole, C. F. *Naturwissenschaften* **1979**, *66*, 423. (f) Schurig, V.; Leyrer, U. *Tetrahedron*: *Asymmetry* **1990**, *1*, 865−868.

(4) (a) Kostyanovsky, R. G.; Rudchenko, V. F. *Dokl. Acad. Nauk SSSR* **1976**, *231*, 878. (b) Kostyanovsky, R. G.; Rudchenko, V. F.; Dyachenko, O. A.; Chervin, I. I.; Zolotoi, A. B.; Atovmyan, L. O. *Tetrahedron* **1979**, *35*, 213−224. (c) Rudchenko, V. F.; Dyachenko, O. A.; Zolotoi, A. B.; Atovmyan, L. O.; Chervin, I. I.; Kostyanovsky, R. G. *Tetrahedron* **1982**, *38*, 961−975. (d) Bucciarelly, M.; Forni, A.; Moretti I.; Torre, G.; Prosyanik, A.; Kostyanovsky, R. G. *J. Chem. Soc., Chem. Commun.* **1985**, 998−999. (g) Shustov, G. V.; Kadorkina, G. K.; Kostyanovsky, R. G.; Rauk, A. *J. Am. Chem. Soc.* **1988**, *110*, 1719−1724. (h) Shustov, G. V.; Varlamov, S. V.; Chervin, I. I.; Aliev, A. E.; Kostyanovsky, R. G.; Kim, D.; Rauk, A. *J. Am. Chem. Soc.* **1989**, *111*, 4210−4215.

(5) (a) Kostyanovsky, R. G.; Rudchenko, V. F.; Shtamburg, V. G.; Chervin, I. I.; Nasibov, S. S. *Tetrahedron* **1981**, *37*, 4245−4254. (b) Rudchenko, V. F.; Chervin, I. I.; Voznesenski V. N.; Nosova, V. S.; Kostyanovsky, R. G. *Izv. Acad. Nauk SSSR* **1988**, 2788−2792.

(6) Tröger, J. *J. Prakt. Chem.* **1887**, *36*, 225−245.

(7) Bag, B. G. *Curr. Sci.* **1995**, *68*, 279−288.

(8) (a) Wilen, S. H.; Qi, J. Z.; Willard, P. G. *J. Org. Chem.* **1991**, *56*, 485−487. (b) Aamouche A.; Devlin, F. J.; Stephens, P. J. *Chem. Commun.* **1999**, 361−362.

(9) Spielman, M. A. *J. Am. Chem. Soc.* **1935**, *57*, 583−585.

(10) Wagner, E. C. *J. Am. Chem. Soc.* **1935**, *57*, 1296−1298.

(11) (a) Sucholeiki, I.; Lynch, V.; Phan, L.; Wilcox,C. S. *J. Org. Chem.* **1988**, *53*, 98−104. (b) Maitra, U.; Bag, B. G. *J. Org. Chem.* **1992**, *57*, 6979−6981. (c) Becker, D. P.; Finnegan, P. M.; Collins, P. W. *Tetrahedron Lett.* **1993**, *34*, 1889−1892. (d) Cerrada, L.; Cudero, J.; Elguero, J.; Pardo, C. *J. Chem. Soc., Chem. Commun.* **1993**, 1713−1714. (e) Crossley, M. J.; Hambley, T. W.; Mackay, L. G.; Try, A. C.; Walton, R. *J. Chem. Soc., Chem. Commun.* **1995**, 1077−1079. (f) Tatibouët, A.; Demeunynck, M.; Lhomme, J. *Synth. Commun.* **1996**, *26*, 4375−4395. (g) Tálas, E.; Margitfalvi, J.; Machytka, D.; Czugler, M. *Tetrahedron: Asymmetry* **1998**, *9*, 4151−4156.

10.1021/ja991184o CCC: $19.00
Published on Web 02/05/2000

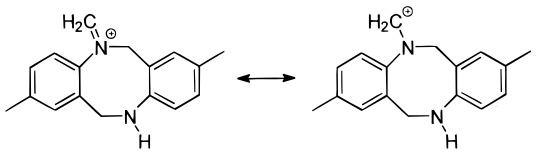

2

Figure 2. Iminium ion of Tröger's base **1**.[17]

1 is due to the presence of two stereogenic nitrogen atoms related by C_2 symmetry. Concomitant inversion of the bridgehead nitrogen atoms is hindered by the bicyclic constitution of **1**. The inherent chirality of **1** was recognized in 1944 by Prelog and Wieland and was proved by resolution into optically active fractions (op = 0.99) by liquid chromatography on a 0.9 m column containing lactose hydrate and subsequent fractional crystallization.[12] Ever since, Tröger's base **1** represents a lucid target for resolution trials by novel innovative chromatographic techniques.[13]

Wilen et al.[8] determined the absolute configuration of dextrorotatory **1** by X-ray crystallography as (+)-(5*S*,11*S*), which was in contradiction to the previous assignment based on the circular dichroism spectrum by the method of exciton chirality.[14] Textbook statements, e.g., *in molecules in which the nitrogen atom is at a bridgehead, pyramidal inversion is of course prevented*[15]*—without breaking a bond*,[16] stimulate further scrutiny concerning the inferred stereointegrity. Indeed, it has been observed that dilute acid causes racemization of **1**, believed to proceed via a bond-breaking step involving an iminium ion **2** (Figure 2). Extrapolating crude published racemiziation data[12] leads to $\Delta G^{\ddagger}_{293\ K} = 98 \pm 2$ kJ/mol. Yet Greenberg et al.[17] did not find any evidence for an iminium ion by NMR studies and their study implied that racemiziation occurs more readily in dilute rather than in concentrated acid.

Tröger's base **1** and derivatives thereof are of recent theoretical and practical interest, e.g., as chiral solvating agents,[8] molecular receptors,[18] and chiral auxiliaries in enantioselective reactions.[19] In an effort to reconsider the proposition that **1** is stereochemical integer, we determined the enantiomerization barrier of Tröger's base by two modern gas-chromatographic techniques.

2. Results and Discussion

In enantioselective dynamic gas chromatography (DGC), enantiomerization[20] gives rise to an interconversion peak profile featuring a plateau between the terminal peaks or peak broadening of the enantiomers,[21,22] separated on a chiral stationary phase. By peak form analysis, kinetic data of interconversion, i.e., the enantiomerization barrier, can be obtained by iterative comparison of experimental and simulated chromatograms.[23,24] The application of the principle of microscopic reversibility requires that the rates of interconversion of the two enantiomers are rendered different in the presence of the chiral stationary phase. This notion is due to the fact that the enantiomers are discriminated, and hence separated, due to a different Gibbs energy ($-\Delta_{B,A}\Delta G = RT \ln(k_B/k_A)$) as shown in Scheme 1.[21]

Scheme 1. Equilibria in a Theoretical Plate[a]

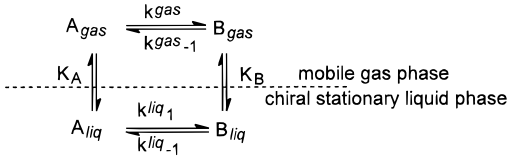

[a] A is the first eluted enantiomer, B is the second eluted enantiomer, *k* represents the rate constant, and *K* represents the distribution constant.

Thus, whereas the second eluted enantiomer is enriched during the chromatographic time scale because it is formed more rapidly than the first eluted enantiomer ($k^{liq}_1 > k^{liq}_{-1}$), no overall deracemiziation occurs as the second eluted enantiomer is depleted to a greater extent due to its longer residence time in the column. While DGC represents a simple technique to assess configurational lability, kinetic data are measured in the presence of the chiral stationary liquid phase leading to different rate constants between the mobile and stationary phases and different forward (k^{liq}_1) and backward (k^{liq}_{-1}) rate constants in the stationary liquid phase, respectively. Recently, we therefore developed the enantioselective stopped-flow multidimensional gas chromatography (sfMDGC) technique[25] which measures enantiomerization barriers in the inert mobile gas phase. It should be noted that, contrary to chiroptical methods, both gas-chromatographic approaches require only nanogram amounts of racemic unresolved mixtures. Yet the prerequisite for both methods is the quantitative on-column separation of the chiral compound into enantiomers in the respective chromatographic setup.

Indeed, the enantiomers of **1** can be resolved by gas chromatography on Chirasil-β-Dex (permethylated β-cyclodextrin linked via a mono(octamethylene) spacer to poly(dimethylsiloxane)[26]), whereby (*S*,*S*)-**1** is eluted first.

Enantiomerization studies in the gas phase are performed by enantioselective stopped flow multidimensional gas chromatography (sfMDGC). The gas chromatograph is equipped with two ovens, a pneumatically controlled six-port valve (Valco), with valve positions A and B, two flame-ionization detectors (FID 1 and FID 2), two separation columns (columns 1 and 3), and a reaction column (column 2). In valve position A injector 1, column 1, and FID 1 are connected, the reaction column 2 is

(12) Prelog, V.; Wieland, P. *Helv. Chim. Acta* **1944**, *27*, 1127−1134.
(13) (a) Kuhn, R.; Hoffstetter-Kuhn, S. *Chromatographia* **1992**, *34*, 505−512 (cf. Figure 2a therein). (b) Okamoto, Y.; Kaida, Y. *J. Chromatogr.* **1994**, *666*, 403−419 (cf. Figure 1 therein). (c) Jung, G.; Hofstetter, H.; Feiertag, S.; Stoll, D.; Hofstetter, O.; Wiesmüller, K.-H.; Schurig, V. *Angew. Chem., Int. Ed. Engl.* **1996**, *35*, 2148−2149 (cf. Figure 1a therein). (d) *J. Mater. Chem.* **1997**, *7*, colored title page of number 10.
(14) Mason, S. F.; Vane, G. W.; Schofield, K.; Wells, R. J.; Whitehurst, J. S. *J. Chem. Soc. B* **1967**, 553−556.
(15) March, J. *Advanced Organic Chemistry*, 4th ed.; John Wiley: New York, 1992; p 100.
(16) Nasipuri, D. *Stereochemistry of Organic Compounds−Principles and Applications*, 2nd ed.; John Wiley: New York, 1994; pp 47−48.
(17) Greenberg, A.; Molinaro, N.; Lang, M. *J. Org. Chem.* **1984**, *49*, 1127−1130.
(18) Cowart, M. D.; Sucholeiki, I.; Bukownik, R. R.; Wilcox, C. S. *J. Am. Chem. Soc.* **1988**, *110*, 6204.
(19) Minder, B.; Schürch, M.; Mallat, T.; Baiker, A. *Catal. Lett.* **1995**, *31*, 143.
(20) (a) Schurig, V.; Bürkle, W. *J. Am. Chem. Soc.* **1982**, *104*, 7573−7580. (b) Reist, M.; Testa, B.; Carrupt, P. A.; Jung, M.; Schurig, V. *Chirality* **1995**, *7*, 396−400. In contrast to the irreversible macroscopic process of racemiziation, enantiomerization is defined as the reversible microscopic conversion of one enantiomer into another.
(21) (a) Craig, L. C. *J. Biol. Chem.* **1944**, *155*, 519. (b) Kallen, J.; Heilbronner, E. *Helv. Chim. Acta* **1960**, *43*, 489−500. (c) Bürkle, W.; Karfunkel, H.; Schurig, V. *J. Chromatogr.* **1984**, *288*, 1−14.
(22) Mannschreck, A.; Zinner, H.; Pustet, N. *Chimia* **1989**, *43*, 165−166.
(23) (a) Jung, M.; Schurig, V. *J. Am. Chem. Soc.* **1992**, *114*, 529−534. (b) Jung, M. Program Simul, No. 620, Quantum Chemistry Program Exchange (QCPE). *QCPE Bull.* **1992**, *3*, 12.
(24) (a) Veciana, J.; Crespo, M. I. *Angew. Chem., Int. Engl. Ed.* **1991**, *30*, 74−77. (b) Wolf, C.; König, W. A.; Roussel, C. *Liebigs Ann.* **1995**, 781−786. (c) Wolf, C.; Hochmuth, D. H.; König, W. A.; Roussel, C. *Liebigs Ann.* **1996**, 357−363. (d) Hochmuth, D. H.; König, W. A. *Liebigs Ann.* **1996**, 947−951.
(25) Schurig, V.; Reich, S. *Chirality* **1998**, *10*, 316.
(26) Schurig, V.; Schmalzing, D.; Schleimer, M. *Angew. Chem., Int. Engl. Ed.* **1991**, *30*, 987−989.

Table 1. Determination of the Enantiomerization Barrier $\Delta G^{\ddagger}_{gas}(T)$ of **1** at Different Temperatures in the Mobile Gas Phase

T (°C)	t (min)	major peak area (%)	k^{gas} (s^{-1})	$\Delta G^{\ddagger}_{gas}$ (kJ mol^{-1})
144.2	15	83.8	2.23E-04	132.8 ± 1.5[a]
149.3	15	81.0	2.65E-04	133.6 ± 0.1
154.2	10	84.8	3.42E-04	134.5 ± 1.5
163.0	15	77.1	5.13E-04	135.7 ± 0.7
172.5	15	83.3	6.90E-04	137.8 ± 1.4
182.4	4	80.3	1.05E-03	139.2 ± 0.1
190.2	2	85.4	1.44E-03	140.4 ± 0.1

[a] Mean deviation of three measurements.

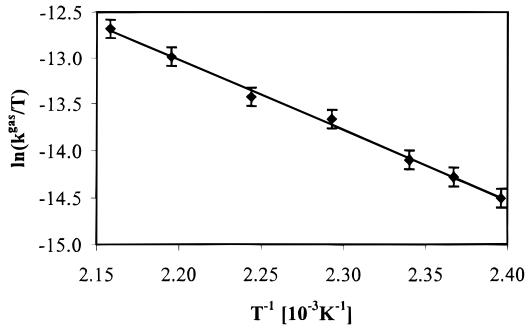

Figure 3. Eyring plot for the determination of $\Delta H^{\ddagger}_{gas}$ and $\Delta S^{\ddagger}_{gas}$ from the enantioselective sfMDGC experiment.

closed, and injector 2, column 3, and FID 2 are connected. In valve position B injector 1, column 1, reaction column 2, column 3, and FID 2 are in line and injector 2 is directly connected to FID 2. The enantiomers of racemic **1** are quantitatively separated in column 1 (Chirasil-β-Dex; cf. Figure 9) in the first oven, in valve position A.

Afterward, either the first or the second eluted (pure) enantiomer is trapped into the reaction column 2 in the second oven via valve position B. For that purpose the reaction column 2 is cooled with liquid nitrogen. The reactor column 2, deactivated with poly(dimethylsiloxane) (1 m × 0.25 mm i.d., 0.002 μm), is quickly heated to the temperature T in valve position A whereby enantiomerization of (*S*,*S*)-**1** or (*R*,*R*)-**1**, respectively, commences. After the contact time t the reaction column 2 is rapidly cooled with liquid nitrogen and the enantiomeric mixture of **1** is transferred at the separation temperature into column 3 in valve position B, where the enantiomers of **1** are separated on Chirasil-β-Dex. The rate constant of enantiomerization is calculated from the observed enantiomeric ratio *er*,[27] the temperature T, and the contact time t according to eq 1.

$$k = \frac{1}{2t} \ln \frac{\mathrm{er} + 1}{\mathrm{er} - 1} \qquad (1)$$

In Table 1 rate constants measured between 144.2 and 190.2 °C are listed. The enantiomer separation of **1** was performed at 135 °C in columns 1 and 3 where interconversion was not observed during chromatography (absence of plateau formation and peak broadening, vide infra). Side products from decomposition or rearrangement, if any, were not observed. The mean values of ln(k/T) were plotted as a function of T^{-1} according to the Eyring equation (Figure 3). A statistical transmission factor of $\kappa = 0.5$ for the *reversible* enantiomerization process has been applied to calculate $\Delta G^{\ddagger}_{gas}$. By a linear regression of the Eyring plot (agreement factor 0.9965) $\Delta H^{\ddagger}_{gas}$ was found to be 62.7 ± 0.3 kJ mol^{-1} and $\Delta S^{\ddagger}_{gas} = -168 \pm 6$ J (K mol)$^{-1}$ in the gas phase.

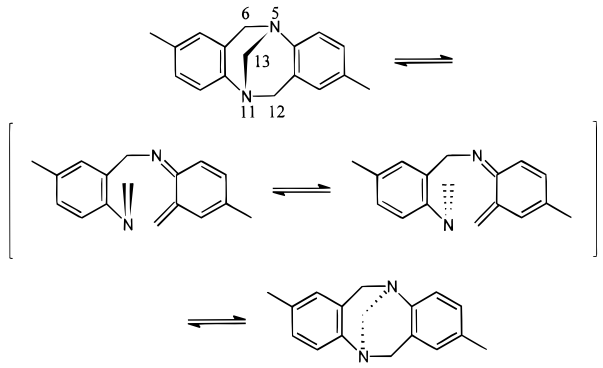

Figure 4. Proposed mechanism of the enantiomerization of **1** via a degenerated retro-hetero-Diels−Alder−hetero-Diels−Alder sigmatropic rearrangement.

The results show that Tröger's base **1** is prone to enantiomerization at ambient temperatures in the inert gas phase. The limited stereointegrity of **1** can also be qualitatively demonstrated by a simple experiment. Heating of neat (*S*,*S*)-**1** in a sealed ampule at 200 °C led to enantiomerization as judged from the decrease of the specific rotation and the decrease of enantiomeric excess *ee* determined by enantioselective gas chromatography on Chirasil-β-Dex.

Thus, the stereointegrity of **1** in the gas phase appears to be lower as intuitively expected. Since care has been taken to deactivate the interior surface of the fused silica column (reaction column 2) by a protective poly(dimethylsiloxane) film, accidental catalytic effects accelerating enantiomerization are believed to be absent in our experiment. Therefore one ampule with neat (*R*,*R*)-**1**, one with neat (*R*,*R*)-**1** and a pulverized fused-silica capillary (the polyamide film was removed), and one with neat (*R*,*R*)-**1** and annealed silica gel were sealed and heated at 200 °C for the same period. There was no increase in the formation of (*S*,*S*)-**1** in the presence of fused silica, but in the presence of silica gel the formation was accelerated in comparison to the ampule without any additives.

Two possible mechanisms of the enantiomerization of **1** in the gas can be envisaged. (i) The mechanism depicted in Figure 4 assumes the rearrangement via a retro-hetero-Diels−Alder ring opening,[28] forming a very reactive intermediate[29] which reacts back by a intramolecular hetero-Diels−Alder ring closure[30] to the enantiomerized product. This mechanism takes into account the preference of the formation of *Schiff bases* (azomethines) rather than amidines between aldehydes and aromatic amines.

Therefore in a first step an optimized structure of (*S*,*S*)-**1** (cf. Figure 5) was calculated with the HyperChem Package rel. 4.0[31] using the MM+ force field[32] followed by the AM1 method.[33] The calculated structure shows that the two six-membered rings

(27) (a) Seebach, D.; Beck, A. K.; Schmidt B.; Wang Y. M. *Tetrahedron* **1994**, *50*, 4363−4384. (b) Schurig, V. *Enantiomer* **1996**, *1*, 139−143. (c) Selke, R. *Enantiomer* **1997**, *2*, 415−419.

(28) (a) Woodward, R. B.; Baer, H. *J. Am. Chem. Soc.* **1944**, *66*, 645. (b) Kwart, H.; King, K. *Chem. Rev.* **1968**, *68*, 415. (c) Smith, G. G.; Kelly, F. W. *Prog. Phys. Org. Chem.* **1971**, *8*, 75. (d) Ripoll, J. L.; Rouessac, A.; Rouessac, F. *Tetrahedron* **1978**, *34*, 19. (e) Lasne, M.-C.; Ripoll, J. L. *Synthesis* **1985**, 121. (f) Ichihara, A. *Synthesis* **1987**, 207.

(29) Fischer, M.; Wagner, F. *Chem. Ber.* **1969**, *102*, 3486−3494.

(30) (a) Carlson, R. G. *Ann. Rep. Med. Chem.* **1974**, *9*, 270. (b) Oppolzer, W. Angew. *Chem. Int. Ed.* **1977**, *16*, 10−18. (c) Brieger, G.; Bennett, J. N. *Chem. Rev.* **1980**, *80*, 67. (d) Fallis, A. G. *Can. J. Chem.* **1984**, *62*, 183. (e) Smith, M. B. *Org. Prep. Proceed. Int.* **1990**, *22*, 315.

(31) HyperChem release 4.0, available from Hypercube Inc., 419 Philip Street, Waterloo, Ontario, Canada N2L 3X2.

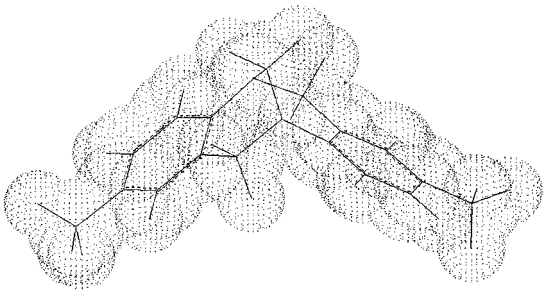

Figure 5. AM1-optimized structure of (*S*,*S*)-**1**.

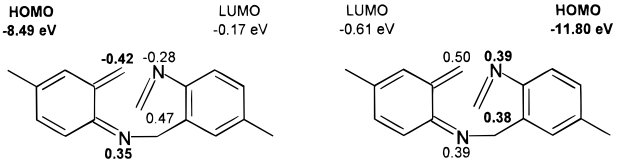

Figure 6. Orbitals of this intramolecular Diels−Alder reaction have been separated due to the rules of Woodward and Hoffmann in HOMO (energy and coefficients printed in bold) and LUMO for the two parts of the molecules, the dienophile and the enophile.

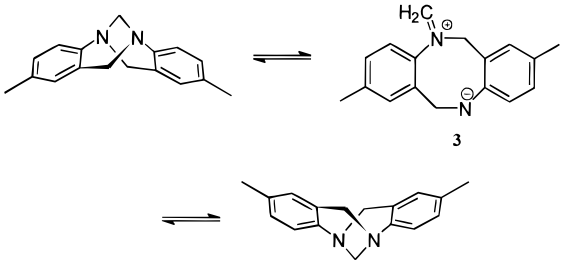

Figure 7. Proposed mechanism of the enantiomerization via zwitterionic intermediate **3**.

of the methanodiazocine system form an extended envelope facilitating ring opening and closure.

In a second step the bonds N11−C12 and N5−C13 of (*S*,*S*)-**1** were broken and double bonds were formed, respectively. The structures were optimized by the MM+ force field followed by the AM1 method. The energies and front orbital MO coefficients from the AM1 method are listed in Figure 6, which confirm the possibility of an intramolecular rearrangement via a hetero-Diels−Alder-reaction.

(ii) The mechanism depicted in Figure 7 assumes the formation of a zwitterionic structure by bond breakage of the methylene bridge, in contrast to acidic catalysis for the interconversion in acidic liquid media.[17] This mechanism involving charge separation is compatible with the observed negative activation entropy as previously reported for the enantiomerization of aziridines and diaziridines.[34] In general an increase of negative entropy is observed for charge separated heterolytic processes.[35] By protonation the enantiomerization rate should increase, because the transition state is stabilized. This agrees

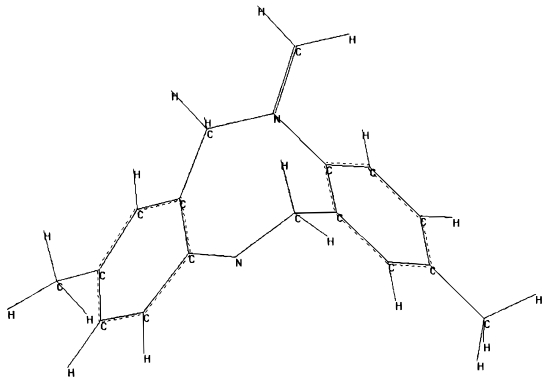

Figure 8. AM1-optimized structure of intermediate **3**.

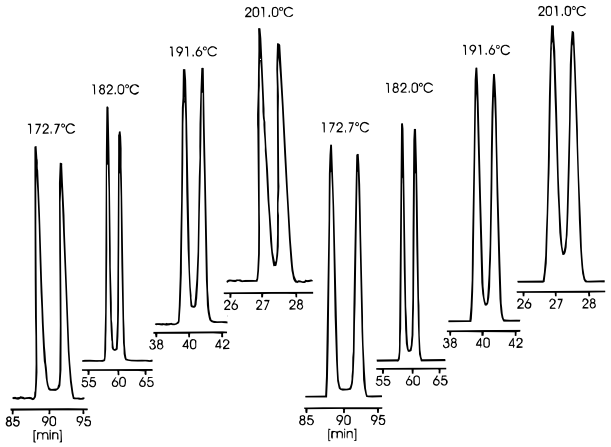

Figure 9. Enantiomerization of **1** at different temperatures: experimental chromatograms (left) vs simulated chromatograms (right).

with the findings of Greenberg et al.[17] that the enantiomerization is favored in dilute acid whereas the enantiomerization is less favored in concentrated acid because of charge repulsion.

To calculate the energy difference between (*S*,*S*)-**1** and the zwitterionic intermediate **3** the bond N5−C13 of (*S*,*S*)-**1** was broken and a double bond was formed, respectively. The structure was optimized by the MM+ force field followed by the AM1 method (the result depicted in Figure 8). The difference of total energy of (*S*,*S*)-**1** and **3** is about 160 kJ mol^{-1}; however, the activation barrier $\Delta G^{\ddagger}$ for the conversion of (*S*,*S*)-**1** to **3** should be considerably higher. Therefore, in the gas phase, this mechanism appears to be less favored.

In a complementary approach, the enantiomerization barrier of **1** was also determined in the chiral stationary liquid phase by dynamic gas chromatography (DGC). Incidentally, enantiomerization studies by DGC have interesting precedents for chiral trivalent nitrogen compounds. The occurrence of characteristic peak profiles produced by nitrogen invertomers has been predicted[3f] and later observed and calculated for the enantiomer separation of 1-chloro-2,2-dimethylaziridine on nickel(II) bis-[(3-heptafluorobutanoyl)-(1*R*)-camphorate] by complexation gas chromatography[21] and of 1-isopropyl-3,3-dimethyldiaziridine and 1,2,3,3-tetramethyldiaziridine on permethyl-β-cyclodextrin by inclusion gas chromatography.[23] The DGC experiment involving Tröger's base **1** and the chiral stationary phase Chirasil-β-Dex shows with increasing temperature from 172.7 to 201.0 °C typical interconversion plateaus (Figure 9).

Rate constants k^{liq} of the enantiomerization of **1** in the stationary liquid phase were calculated by simulation of the chromatograms with the new program ChromWin,[36] using the theoretical plate model, as depicted in Scheme 1.

(32) Allinger, N. L. *J. Am. Chem. Soc.* **1977**, *99*, 8127.

(33) (a) Dewar, M. J. S.; Zoebisch, E. G.; Healy E. F.; Stewart, J. J. P. *J. Am. Chem. Soc.* **1985**, *107*, 3902. (b) Dewar, M. J. S.; Dieter, K. M. *J. Am. Chem. Soc.* **1986**, *108*, 8075. (c) Stewart, J. J. P. *J. Comput. Aided Mol. Des.* **1990**, *4*, 1.

(34) (a) Shustov, G. V.; Varlamov, S. V.; Shibaev, A. Yu.; Puzanov, Yu. V.; Kostyanovsky, R. G. *Izv. Acad. Nauk SSSR, Ser. Khim.* **1989**, 1816−1819. (b) Shustov, G. V.; Denisenko, A. Yu.; Shibaev, A. Yu.; Puzanov, Yu. V.; Kostyanovsky, R. G. *Khim. Phys.* **1989**, *8*, 366.

(35) (a) Frost, A. A.; Pearson, R. G. *Kinetics and Mechanism*, 2nd ed.; John Wiley: New York, 1961; p 135. (b) Hermann, H.; Huisgen, R.; Mader, H. *J. Am. Chem. Soc.* **1971**, *93*, 1779. (c) Yankee, E. W.; Bader, F. D.; Howe, N. E.; Cram, D. J. *J. Am. Chem. Soc.* **1973**, *95*, 4210.

This model describes the chromatographic separation as a discontinuous process,[21] assuming that all steps proceed repeatedly in separate uniform sections of a multicompartmental column with N theoretical plates considered as chemical reactor. Three steps (i, ii, iii) take place in every plate (cf. Scheme 1):

(i) The distribution of the enantiomers A and B between mobile gas phase (gas) and the stationary liquid phase (liq) is determined according to the eqs 2 and 3, where A_{gas}, B_{gas}, A_{liq},

$$A_{gas} = \frac{1}{1+k'_A}(A^\circ_{gas} + A^\circ_{liq}) \quad B_{gas} = \frac{1}{1+k'_B}(B^\circ_{gas} + B^\circ_{liq}) \tag{2}$$

$$A_{liq} = \frac{k'_A}{1+k'_A}(A^\circ_{gas} + A^\circ_{liq}) \quad B_{liq} = \frac{k'_B}{1+k'_B}(B^\circ_{gas} + B^\circ_{liq}) \tag{3}$$

and B_{liq} are the amounts of enantiomers A and B at equilibrium, A°_{gas}, B°_{gas}, A°_{liq}, and B°_{liq} are the amounts of A and B before the equilibrium, and k'_A and k'_B are the retention factors of A and B, calculated from the total retention time t_R and the mobile phase hold-up time t_M according to $k' = (t_R - t_M)/t_M$.

(ii) The reversible enantiomerization process between the enantiomers during the residence time $\Delta t = t_M/N$ in the chiral stationary liquid phase and in the achiral mobile gas phase in a theoretical plate is determined by the respective rate constants. The forward and backward rate constants k^{gas} in the mobile phase are equal (the equilibrium constant is $K^{gas} = 1$), whereas the equilibrium constant in the chiral stationary liquid phase depends on the two phase distribution constants (=partition coefficients) K_A and K_B according to the principle of microscopic reversibility:[21]

$$K^{liq} = \frac{k_1^{liq}}{k_{-1}^{liq}} = \frac{K_B}{K_A} = \frac{k'_B}{k'_A} \tag{4}$$

This implies that the backward rate constant k_{-1}^{liq} is already determined for given values of k_1^{liq}, k'_A, and k'_B.

The reversible first-order kinetics is described by

$$\frac{dx}{dt} = k_1^{liq}([A_0] - [X]) - k_{-1}^{liq}([B_0] + [X]) \tag{5}$$

where the amount [X] is the change of A and B. Equation 5 is solved by integration, using the following initial conditions:

$$[A] = \frac{k_{-1}^{liq}}{k_1^{liq} + k_{-1}^{liq}}([A_0] + [B_0]) + \frac{k_1^{liq}[A_0] - k_{-1}^{liq}[B_0]}{k_1^{liq} + k_{-1}^{liq}} \exp[-(k_1^{liq} + k_{-1}^{liq})\Delta t] \tag{6}$$

The amount of [B] is calculated from the mass balance due to $[A_0] + [B_0] = [A] + [B]$.

Assuming that the rate constant in the mobile and stationary phase is equal in a first approximation, the overall or apparent rate constant is derived:

$$k_1^{app} = \frac{1}{1+k'_A} k^{gas} + \frac{k'_A}{1+k'_A} k_1^{liq}$$

$$k_{-1}^{app} = \frac{1}{1+k'_B} k^{gas} + \frac{k'_B}{1+k'_B} k_{-1}^{liq} \tag{7}$$

(iii) After the two steps i and ii proceeded, the content of the mobile phase is shifted to the subsequent theoretical plate, whereas the stationary phase is retained. While the given amount of the enantiomers is initially introduced in the first theoretical plate, the content of the mobile phase of the last theoretical plate is finally recorded as a chromatogram featuring an interconversion profile over the time t.

Since the residence time of the enantiomers in the gas phase is usually low (large k'), the contribution to the overall enantiomerization has previously been neglected as no such data were available.[21,23] In the present work, however, the rate constant in the gas phase obtained from the sfMDGC experiment (vide supra) was used as a key value for enantiomerization in the mobile phase k^{gas}. In Table 2 the data for simulation are listed.

By a linear regression of the Eyring plot (agreement factor 0.9856) $\Delta H^\ddagger_{liq}$ was found to be 48.9 kJ mol^{-1} and $\Delta S^\ddagger_{liq} = -231 \pm 8$ J (K mol)$^{-1}$ in the stationary phase. Assuming the same rate constant in the stationary and mobile phases (vide supra), the apparent rate constant k_{app} and Gibb's energy $\Delta G^\ddagger_{app}$ are also obtained from the simulation experiment. In Figure 10 the enantiomerization barriers $\Delta G^\ddagger_{gas}$, $\Delta G^\ddagger_{liq}$, and $\Delta G^\ddagger_{app}$ of **1** are plotted against different temperatures.

When the data obtained by enantioselective sfMDGC in the gas phase are compared with that by enantioselective DGC in the two-phase gas-liquid system, a higher enantiomerization barrier is observed in the latter. This unexpected result implies that the Gibb's energy of the transition state $\Delta G^\ddagger$ increases in the presence of the chiral stationary phase Chirasil-β-Dex.

Enantiomerization in the stationary phase should be separated into two contributions.[23] Whereas a nonenantioselective process commences in the achiral matrix poly(dimethylsiloxane) (uncomplexed state), an enantioselective process takes place in the presence of the cyclodextrin selector (complexed state). To estimate the contribution of the dissolved and complexed state to the rate constant in the stationary phase, the concept of the retention increment R' [21,39] (cf. Scheme 2) has been applied.[23a]

The retention increment R' (i.e. $R' = (k'/k'_{achiral}) - 1$), is easily accessible experimentally and is obtained by relating the retention parameters on a separation column containing the cyclodextrin selector (CD) linked to poly(dimethylsiloxane) with those observed on an achiral reference column containing only the poly(dimethylsiloxane) solvent devoid of the cyclodextrin selector (CD). The retention increment R' is a measure for the selective interaction between the enantiomer and the cyclodextrin selector (CD), as governed by the formation constant $K_{CD,A}$ and $K_{CD,B}$,[39] respectively. The retention increment R' is derived as $R'_A = K_{CD,A} m_{CD}$ (m_{CD} refers to the temperature-independent molality[39a] of the cyclodextrin selector (CD) in the stationary liquid phase). R' represents the fraction of the complexed (com) vs uncomplexed (uncom) enantiomer A, according to the residence time $1/(R'_A + 1)$ and $R'_A/(R'_A + 1)$, in the stationary

(36) Trapp, O. ChromWin 99 is available from the authors upon request as an executable program, running under Windows 3.11/95/98/NT.

(37) Gonzales, F. R. *J. Chromatogr. A* **1999**, *832*, 165−172.
(38) (a) Kramer, R. *J. Chromatogr.* **1975**, *107*, 241−252. (b) Cremer, E.; Kramer, R. *J. Chromatogr.* **1975**, *107*, 253−263.
(39) (a) Schurig, V.; Chang, R. C.; Zlatkis, A.; Feibush, B. *J. Chromatogr.* **1974**, *99*, 147−171. (b) Jung, M.; Schmalzing, D.; Schurig, V. *J. Chromatogr.* **1991**, *552*, 43−57. (c) Schurig, V. In *Chromatographic Separations Based on Molecular Recognition*; Jinno, K., Ed.; Wiley-VCH: New York, 1997; pp 371−418. (d) Schurig, V.; Juza, M. *J. Chromatogr. A* **1997**, *757*, 119−135.

Table 2. Results of the DGC Experiment and Simulations[a]

T (°C)	t_M (min)	t_RA (min)	t_RB (min)	N	$\Delta G^{\ddagger}_{gas}$ (kJ mol^{-1})	k^{gas} (s^{-1})	$\Delta G^{\ddagger}_{liq}$ (kJ mol^{-1})	k_1^{liq} (s^{-1})	$\Delta G^{\ddagger}_{app}$ (kJ mol^{-1})	k_1^{app} (s^{-1})
160.0	1.258	166.12	174.88	70 000	135.6	2.02E-04	149.0	4.91E-06	148.0	6.41E-06
172.7	1.167	89.61	93.31	72 000	137.7	3.43E-04	151.9	7.45E-06	150.2	1.18E-05
182.0	1.180	58.03	59.96	68 000	139.3	4.93E-04	154.0	9.96E-06	151.4	1.98E-05
191.6	1.285	39.70	40.75	71 000	140.9	7.10E-04	156.3	1.33E-05	152.4	3.59E-05
201.0	1.248	27.03	27.60	78 000	142.5	1.00E-03	158.4	1.74E-05	153.4	6.28E-05

[a] t_M: mobile phase hold-up time, measured from the (essentially unretained) methane peak.[37] N: mean number of effective plates calculated from $t_R - t_M$ for the two terminal peaks of the enantiomers and by doubling the outer parts[38] of the peak width at half-height. t_R: total retention time of the first and second eluted enantiomer, respectively.

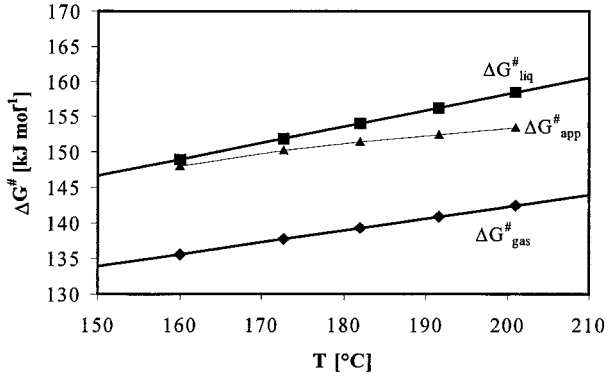

Figure 10. Enantiomerization barrier $\Delta G^{\ddagger}$ at different temperatures in the stationary liquid and mobile gas phases ($\Delta G^{\ddagger}_{gas}$, enantiomerization barrier in the mobile gas phase obtained by enantioselective sfMDGC; $\Delta G^{\ddagger}_{liq}$, calculated enantiomerization barrier in the stationary liquid phase from the sfMDGC and DGC experiment; $\Delta G^{\ddagger}_{app}$, apparent enantiomerization barrier obtained by enantioselective DGC).

Scheme 2. Equilibria in a Theoretical Plate Involving Achiral and Chiral Contributions to Retention in the Stationary Phase[a]

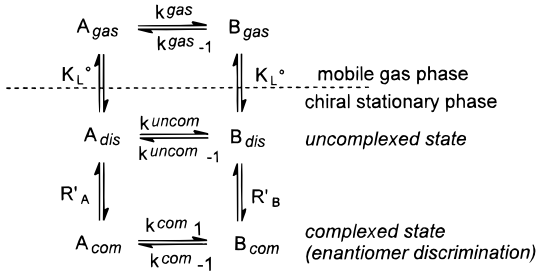

[a] (K_L° denotes the distribution equilibrium between pure A_{gas} and A_{dis} (and B, respectively).

phase.[39] A related expression refers to enantiomer B. This leads to equations analogous to eq 6:

$$k_1^{liq} = \frac{1}{1+R'_A} k^{uncom} + \frac{R'_A}{1+R'_A} k_1^{com}$$

$$k_{-1}^{liq} = \frac{1}{1+R'_B} k^{uncom} + \frac{R'_B}{1+R'_B} k_{-1}^{com} \qquad (8)$$

In Table 3 the data of the retention increment R' and the thermodynamic enantioselectivity $-\Delta_{B,A}\Delta G_{CD}$ (calculated by the equation $-\Delta_{B,A}\Delta G_{CD} = RT \ln(R'_B/R'_A)$) are summarized.

From the linear fit of the van't Hoff plot of $\ln(R'_B/R'_A)$ against $1/T$ (agreement factor 0.9733) $\Delta_{B,A}\Delta H_{CD}$ and $\Delta\ \Delta S_{CD}$ were calculated. $\Delta_{B,A}\Delta H_{CD}$ was found to be 1.6 kJ mol^{-1} and $\Delta\Delta S_{CD} = 3.2$ J (K mol)$^{-1}$. At the calculated isoenantioselective temperature $T_{iso} = 510$ K ($T_{iso} = \Delta_{B,A}\Delta H_{CD}/\Delta_{B,A}\Delta S_{CD}$) peak

Table 3. Experimental Retention Increment R' of the Enantiomers of **1** on Chirasil-β-Dex

	T (°C)								
	120	130	140	150	160	170	180	190	200
R'_A	1.92	1.92	1.56	1.43	1.40	1.29	1.26	1.25	1.12
R'_B	2.14	2.12	1.72	1.56	1.51	1.38	1.33	1.30	1.15
$-\Delta_{B,A}\Delta G_{CD}$ (J mol^{-1})	369	342	336	312	276	244	201	153	106

coalescence[40] is predicted (no enantiomer separation of **1** is possible).

To estimate values for the reaction rate of the complexed and uncomplexed state, arbitrary ratios of k_{com}/k_{uncom} have been obtained from eq 7. The results are represented in Table 4, and the Gibb's energy of enantiomerization is given at 298.15 K (cf. Figure 11).

Figure 11 shows that the enantiomerization barrier $\Delta G^{\ddagger}$ of **1** in the uncomplexed state is in the reasonable range of about 115−120 kJ mol^{-1} and for the complexed state in the reasonable range of about 120−123 kJ mol^{-1}. The increased latter values are attributed to a lower activation entropy, which implies a highly ordered and constrained transition state in the presence of the chiral stationary phase Chirasil-β-Dex.[26] A similar phenomenon has been observed previously in dynamic high-performance liquid chromatography (DHPLC).[41]

3. Experimental Section

The enantiomers of Tröger's base, i.e., (±)-2,8-dimethyl-6*H*,12*H*-5,11-methanodibenzo[*b*,*f*][1,5]diazocine, (+)-2,8-dimethyl-6*H*,12*H*-5,11-methanodibenzo[*b*,*f*][1,5]diazocine, and (−)-2,8-dimethyl-6*H*,12*H*-5,11-methanodibenzo[*b*,*f*][1,5]diazocine, were obtained from Aldrich.

3.1. Stopped-Flow MDGC. Stopped-flow MDGC was performed on a Siemens Sichromat 2 gas chromatograph equipped with two ovens, a pneumatically controlled six-port valve (Valco), a cooling trap in oven 2 for use with liquid nitrogen, a liquid injector (250 °C), an on-column injector (40 °C), and two flame-ionization detectors (250 °C). The whole process is monitored by a control computer. For separation of **1** two fused-silica columns (columns 1 and 3) coated with Chirasil-β-Dex[26] (5 m × 0.25 mm i.d., 0.2 μm film thickness, 135 °C) in oven 1 were employed. As reaction column 2, a deactivated fused silica column (1 m × 0.25 mm i.d.), coated with poly(dimethylsiloxane) (0.002 μm film thickness), was used. Helium was employed as the inert carrier gas.

3.2. Dynamic GC. Enantiomer separation of **1** was performed on a Siemens Sichromat 2, equipped with a liquid injector (250 °C), a flame-ionization detector (250 °C), and a Shimadzu C-R 6A integrator, employing a fused-silica column (25 m × 0.25 mm i.d) coated with Chirasil-β-Dex[26] (0.4 μm film thickness). Helium was used as the inert carrier gas. The measurements were repeated three times at each temperature.

(40) Schurig, V.; Ossig, A.; Link, R. *Angew. Chem., Int. Ed. Engl.* **1989**, *28*, 194−196.

(41) Gasparrini, F.; Misiti, D.; Pierini, M.; Villani, C. *Tetrahedron: Asymmetry* **1997**, *8*, 2069−2073.

Table 4. Eyring Activation Parameters of the Enantiomerization of **1** Obtained via Separation of the Rate Constant between the Complexed and Uncomplexed State in the Liquid Phase

	k_{com}/k_{uncom}								
	0.0001	0.05	0.1	0.3	0.5	0.7	0.9	1	2
$\Delta H^{\ddagger}_{uncom}$ (kJ mol^{-1})	41.5	42.3	43.0	45.1	46.6	47.7	48.6	48.9	51.0
$\Delta S^{\ddagger}_{uncom}$ (J (K mol)$^{-1}$])	−246.3	−245.0	−244.0	−240.9	−239.0	−237.8	−237.0	−236.7	−235.8
$\Delta G^{\ddagger}_{dis}$ (kJ mol^{-1})[a]	114.9	115.4	115.7	117.0	117.9	118.6	119.2	119.5	121.3
$\Delta H^{\ddagger}_{com}$ (kJ mol^{-1})	41.5	42.3	43.0	45.1	46.6	47.7	48.6	48.9	51.0
$\Delta S^{\ddagger}_{com}$ (J (K mol)$^{-1}$)	−322.8	−269.9	−263.1	−250.9	−244.8	−240.8	−237.9	−236.7	−230.0
$\Delta G^{\ddagger}_{com}$ (kJ mol^{-1})[a]	137.8	122.8	121.4	120.0	119.6	119.5	119.5	119.5	119.6

[a] At 298.15 K.

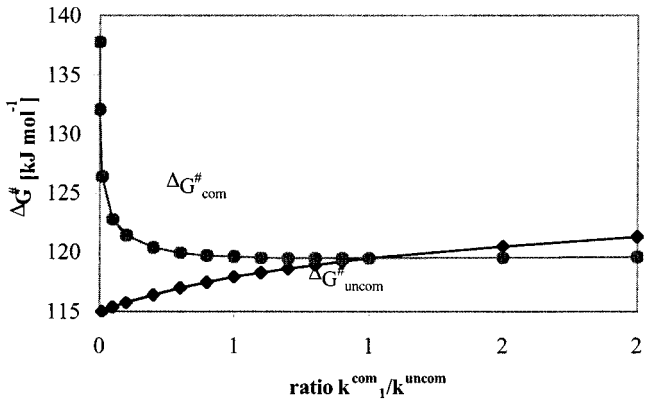

Figure 11. Plot of the ratio k_1^{com}/k^{uncom} versus $\Delta G^{\ddagger}$ at 298.15 K.

3.3. Computer Simulation. Simulations of the experimental chromatograms were performed with the new program ChromWin 99,[36] which is compatible both with the discontinuous plate model[21] and the stochastic model,[42] running under Windows on a IBM-compatible personal computer. The effective plate number N_{eff}, total retention times t_R, and mobile phase hold-up time t_M (using methane) of the column were determined experimentally. The initial amounts of the enantiomers were equal (racemate). Given the rate constant k^{gas} in the mobile phase from the stopped-flow MDGC experiment, the simulation was performed for different values of the rate constant k_1^{liq} in the stationary phase (k_{-1}^{liq} being calculated from k_1^{liq} according to the principle of microscopic reversibility) in order to find the best agreement of the simulated and experimental elution profiles. A statistical transmission factor κ of 0.5 has been used in the Eyring equation to calculate $\Delta G^{\ddagger}$, due to the definition of enantiomerization as a reversible microscopic conversion.

$$k = \kappa \frac{k_B T}{h} e^{-\Delta G^{\ddagger}/RT}$$

3.4. Determination of the Retention Increment *R′*. The retention increments R' were determined by using an achiral reference column coated with poly(dimethylsiloxane) (SE 30, 25 m × 0.25 mm i.d., 0.4 μm film thickness) and a fused-silica column coated with Chirasil-β-Dex[26] (25 m × 0.25 mm i.d., 0.4 μm film thickness). The injected racemate of **1** was transferred simultaneously with a Y-glass-connector onto the two separation columns. *n*-Heptadecane was co-injected as a reference standard and methane as void-column marker, as previously described in detail.[39d] A Carlo Erba Fractovap 2350 gas chromatograph equipped with a liquid-split-injector (250 °C) and two flame-ionization detectors (250 °C) was used. Helium was used as the inert carrier gas.

3.5. Molecular Mechanics Calculations. Calculations were performed with the HyperChem package release 4.0.[31] The initial structures were model built, and the first energy minimizations were carried out with the MM+[32] force field. After that the obtained structure were refined with the semiempirical method AM1,[33] using the standard parameters of the package. All atomic positions were optimized with the conjugate gradient method (Polak−Ribiere) until the RMS gradient reached a value of 0.1 kcal Å^{-1} mol^{-1}.

Acknowledgment. This work was supported by the Deutsche Forschungsgemeinschaft and Fonds der chemischen Industrie. We thank Prof. Kostyanovsky, Russian Academy of Science, for valuable discussions. This contribution is dedicated to Professor Günther Wulff, Institute for Organic Chemistry at the Heinrich Heine University of Duesseldorf, Germany, on the occasion of his 65th anniversary.

JA991184O

(42) Keller, H. A.; Giddings, J. C. *J. Chromatogr.* **1960**, *3*, 205.